

Supporting Information

Selective recognition of the amyloid marker single thioflavin T using DNA origami-based gold nanobipyramid nanoantennas

Charanleen Kaur, Vishaldeep Kaur, Shikha Rai, Mridu Sharma and Tapasi Sen*

Institute of Nano Science and Technology, Sector-81, Mohali, Punjab -140306, India

*E-mail: tapasi@inst.ac.in

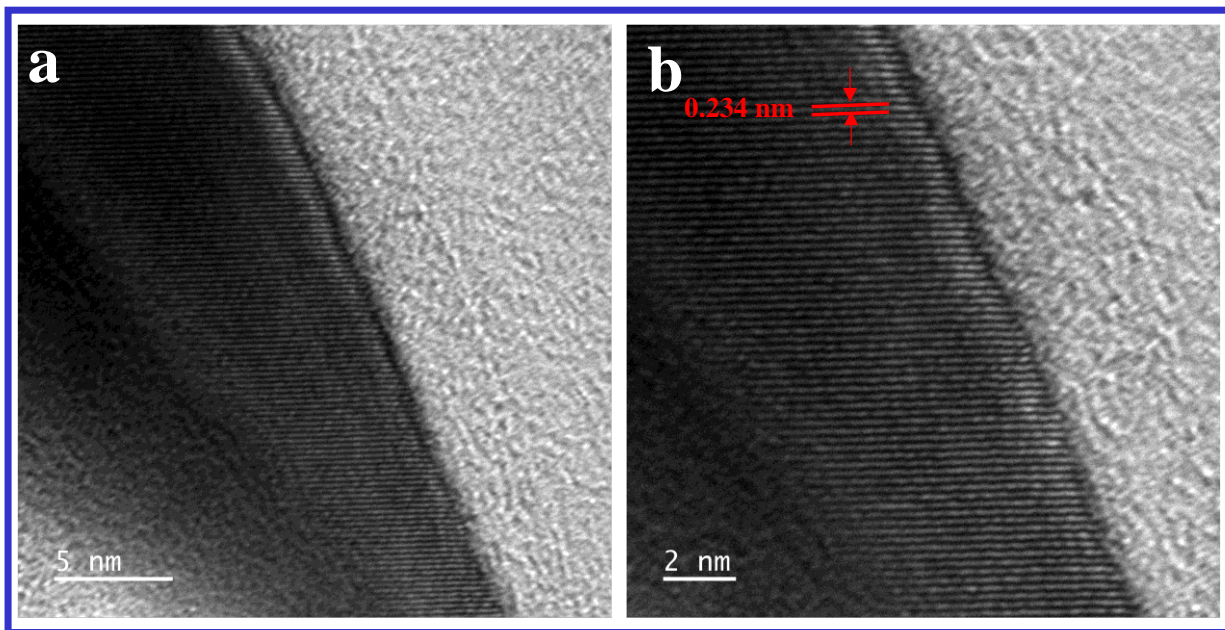


Figure S1. (a) and (b) HRTEM images of Au NBP.

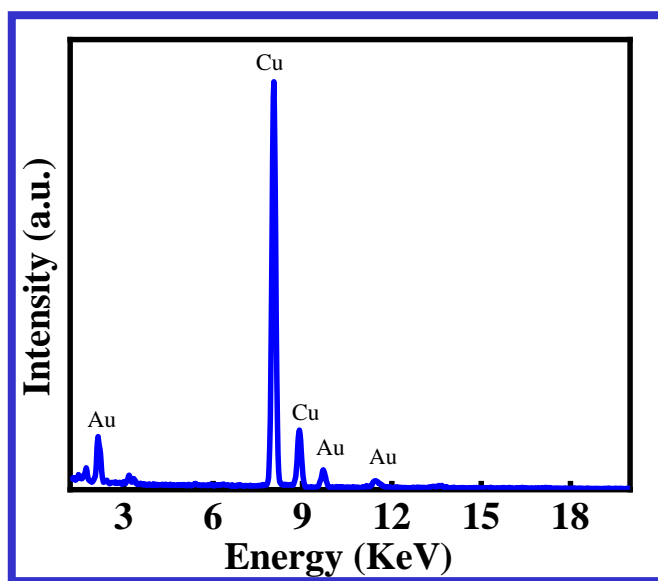


Figure S2. EDX spectrum of Au NBPs.

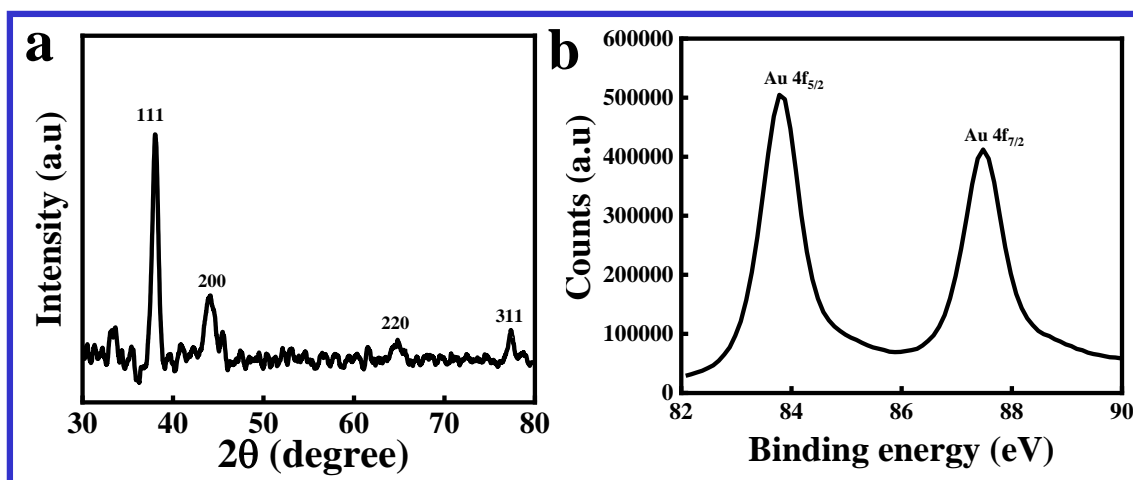


Figure S3. (a) XRD patterns, and (b) XPS spectrum of Au NBPs.

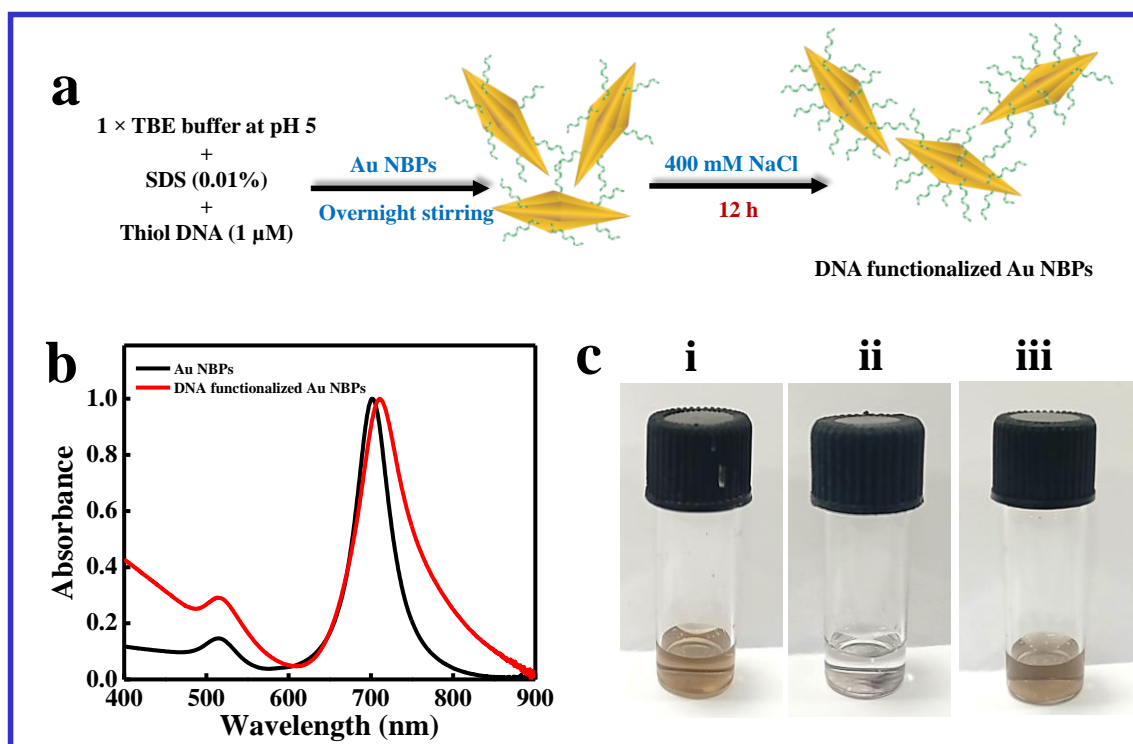


Figure S4. (a) Schematic illustration of DNA functionalization of Au NBPs, (b) Overlay UV-Vis spectra of Au NBPs and DNA functionalized Au NBPs, (c) Pictorial depiction of (i) Au NBPs, (ii) Au NBPs in presence of PBS, 500 mM NaCl, and (iii) DNA functionalized Au NBPs in presence of PBS, 500 mM NaCl.

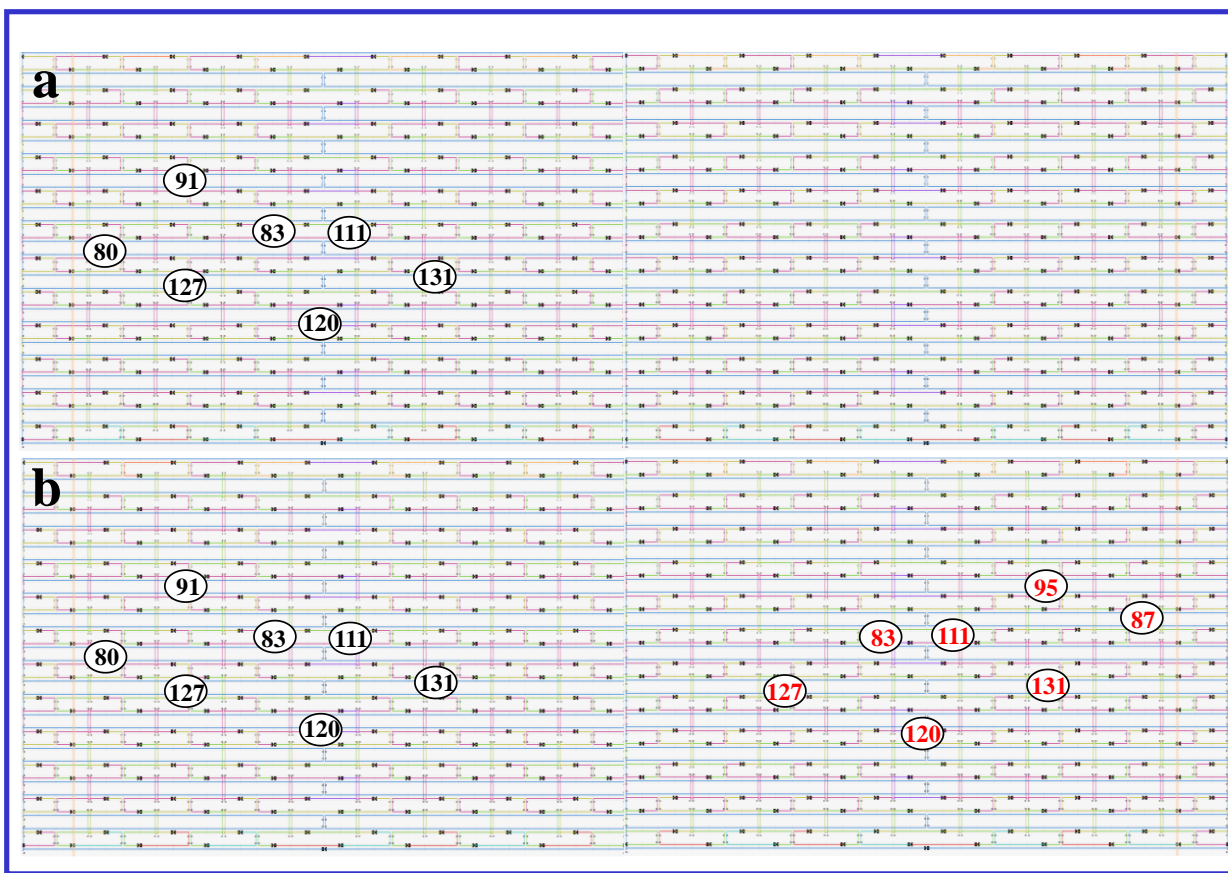


Figure S5. Capturing strands position for immobilization of Au NBPs (a) monomer, and (b) dimer on DNA origami.

Table S1. Thiol modified DNA sequences.

Name	Sequence 5' to 3'
1	5'-SH- CGTCGTATTCGATAGCTTAG
2	5'-SH-TTGGTGGTGGTGGTGGTGGT

Table S2. Modified staple strand sequences on DNA origami.

Na me	Sequence 5' to 3'
Monomer A	
80	AAACAGTTGATGGCTTAGAGCTTATTTAAATACCACCACCACCA
83	AAGAGGAACGAGCTTCAAAGCGAAGATACATTCACCACCACCACCA
91	TACCTTTAAGGTCTTTACCCTGACAAAGAAGTCCACCACCACCACCA
111	TTTCATTTGGTCAATAACCTGTTTAATCAATACCACCACCACCACCA
120	GCGTTATAGAAAAGCCTGTTTAGAAGGCCGCCACCACCACCACCA
127	GGTAGCTAGGATAAAAATTTTTAGTTAACATCCCACCACCACCACCA

131	AGGCGTTACAGTAGGGCTTAATTGACAATAGACCACCACCACCA
Monomer B	
83	AAGAGGAACGAGCTTCAAAGCGAAGATACATTCTAAGCTATCGA
87	CTTTACAGTTAGCGAACCTCCCGACGTAGGAACTAAGCTATCGA
95	TATTTTGCTCCCAATCCAAATAAGTGAGTTAACTAAGCTATCGA
111	TTTCATTTGGTCAATAACCTGTTTAATCAATACTAAGCTATCGA
120	GCGTTATAGAAAAAGCCTGTTTAGAAGGCCGGCTAAGCTATCGA
127	GGTAGCTAGGATAAAAATTTTTAGTTAACATCCTAAGCTATCGA
131	AGGCGTTACAGTAGGGCTTAATTGACAATAGACTAAGCTATCGA
G-rich Branching staple	
106	GCTAAATCCGACAAAATTTTAGTCCGTGGTAGGGCAGGTTGGGGTGACTTTTT GGTAAAGTAGAGAATA

Table S3. Biotin modified staple strand sequences on DNA origami.

Name	Sequence 5' to 3'
Bio-11	Biotin- TTGAGAATAGCTTTTGCGGGATCGTCGGGTAGCA
Bio-27	Biotin-TTGGAAGCGACCAGGCGGATAAGTGAATAGGTG
Bio-188	Biotin- TTTGGTTTTTAACGTCAAAGGGCGAAGAACCATC
Bio-205	Biotin- GCCAACAGTCACCTTGCTGAACCTGTTGGCAA

Table S4. Staple strand sequences for control measurements.

Name	Sequence 5' to 3'
DNA 1	GCTAAATCCGACAAAAGGTAAAGTAGAGAATATTTT
DNA 2	GCTAAATCCGACAAAAGGTAAAGTAGAGAATAATTGTATGAGTAGAGA TTTGTAAGAGCTGTTAGTTAGCTCGCTCAGCTAATAGTTGCCACACAA CGTCAAAATTAGAGAACGGTCGTAACATTATCG

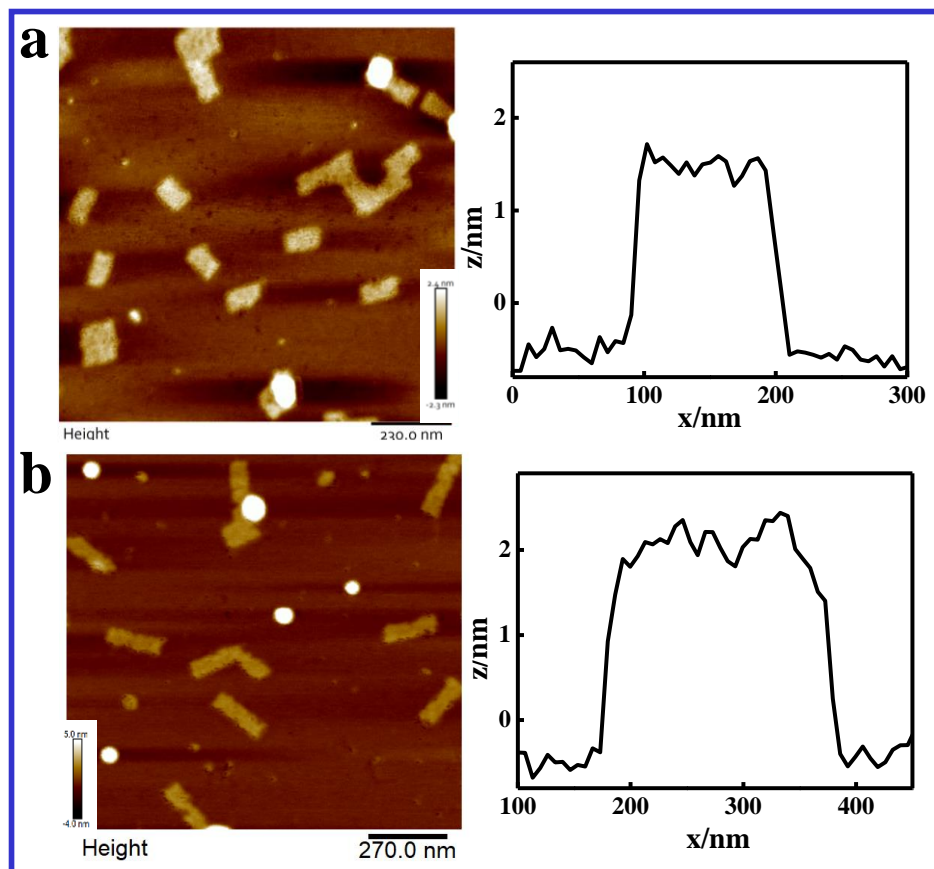


Figure S6. AFM images of DNA origami (a) monomer, and (b) dimer with corresponding height profiles.

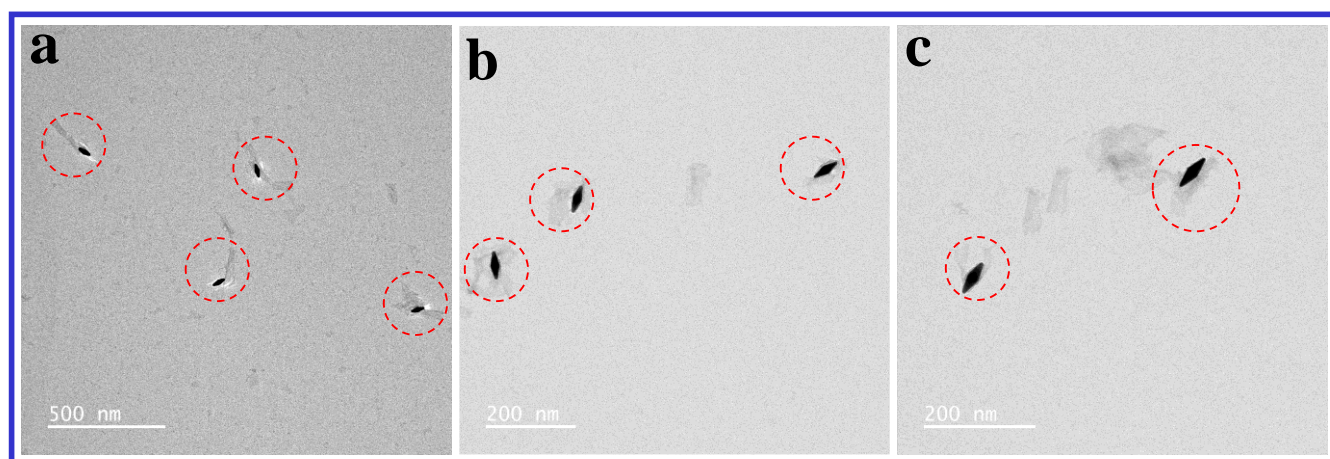


Figure S7. (a), (b), and (c) TEM images of Au NBP monomer on DNA origami.

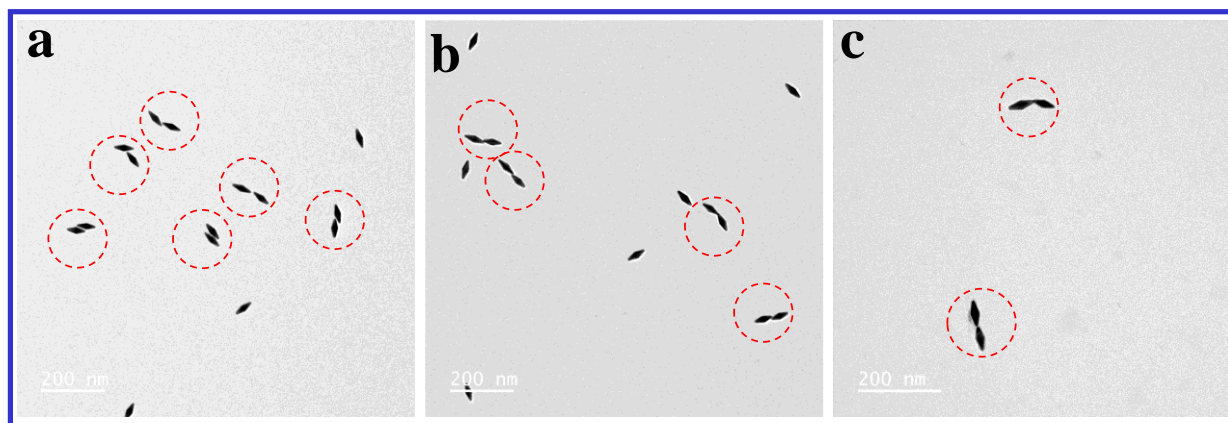


Figure S8. (a), (b), and (c) TEM images of Au NBPs dimer on DNA origami.

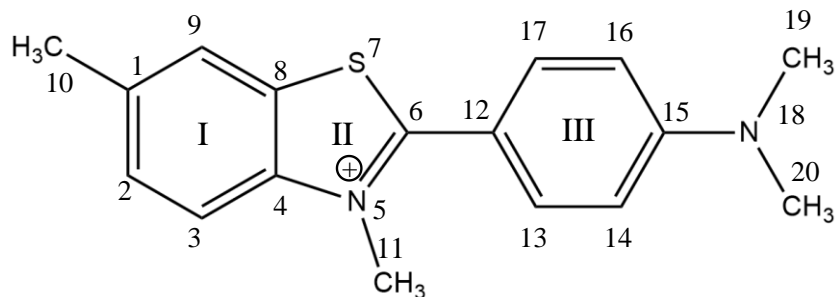


Figure S9. Structure of ThT.

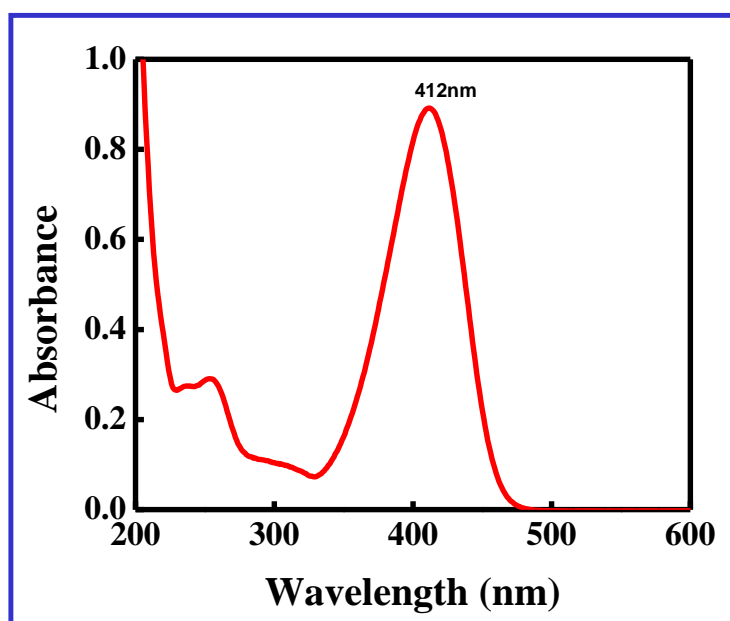


Figure S10. UV-Vis spectrum of ThT.

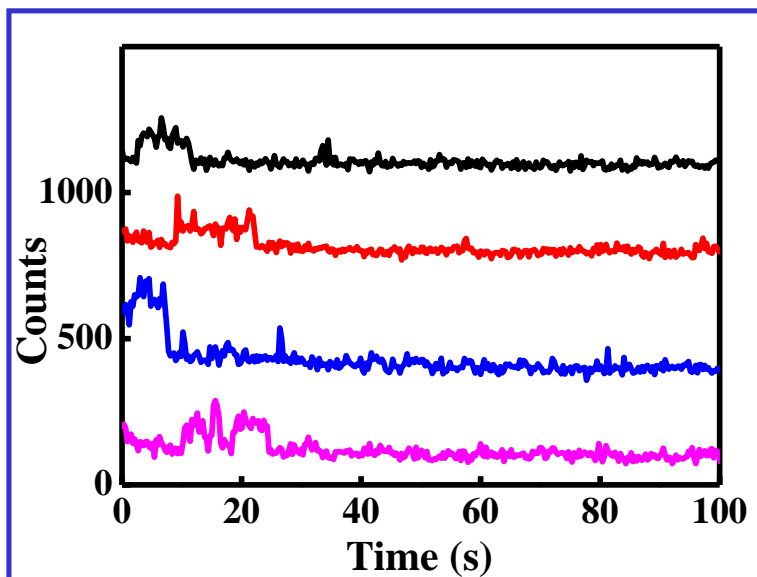


Figure S11. Time trace profiles of ThT dye molecule on DNA origami.

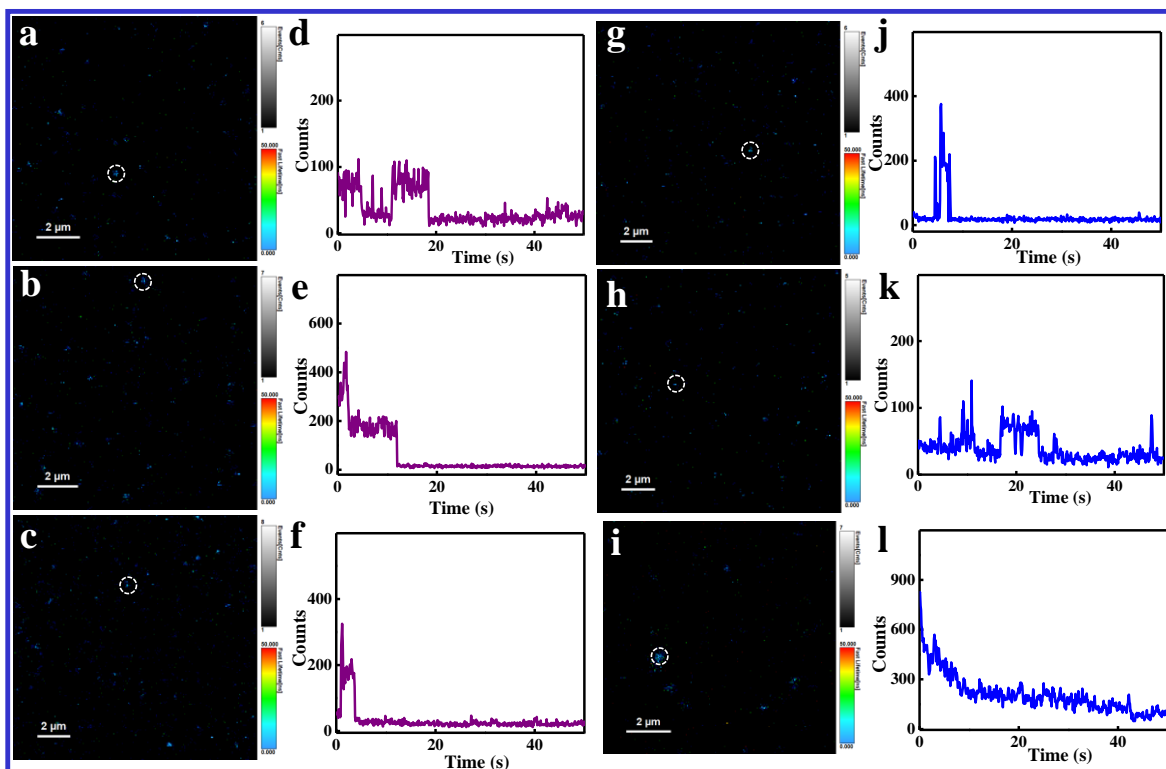


Figure S12. (a, b, c), and (g, h, i) FLIM images, and (d, e, f), and (j, k, l) corresponding time trace profiles for 40 nM ThT solution using Au NBPs monomer, and dimer on DNA origami, respectively.

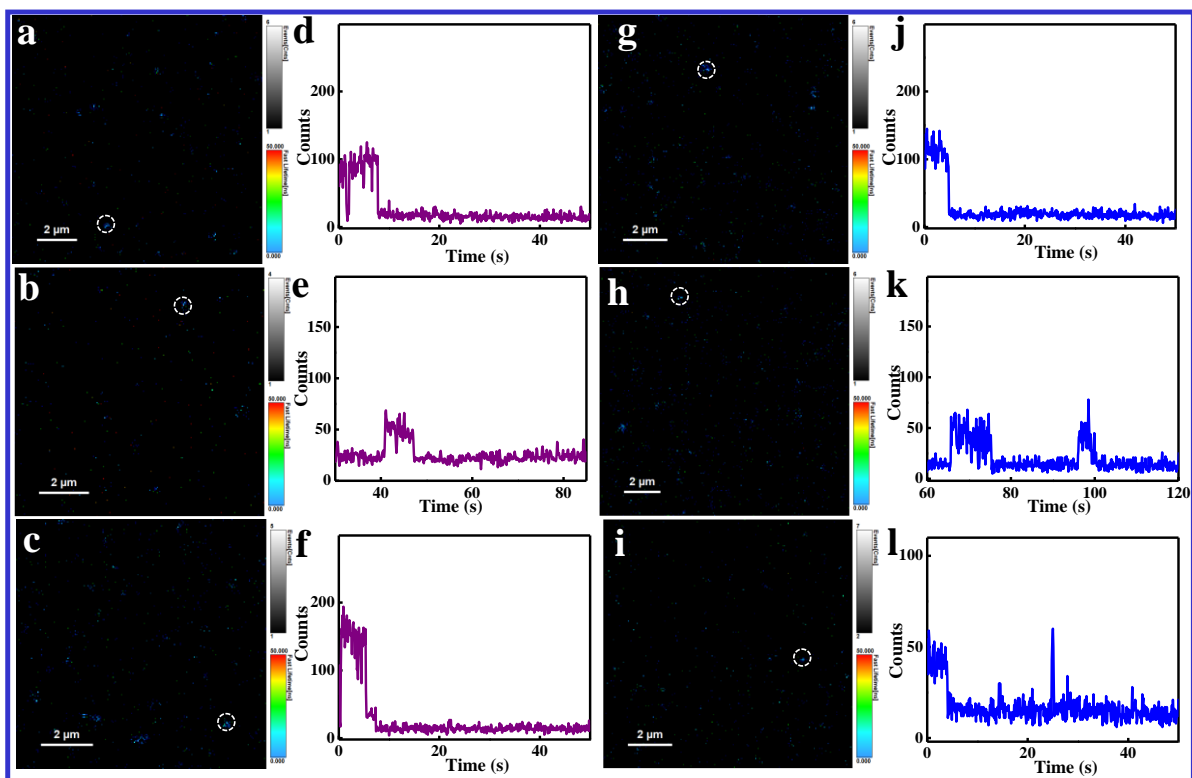


Figure S13. (a, b, c), and (g, h, i) FLIM images, and (d, e, f), and (j, k, l) corresponding time trace profiles for 20 nM ThT solution using Au NBPs monomer, and dimer on DNA origami, respectively.

Table S5. Calculation of distribution of number of ThT molecules on Au NBPs nanoantenna.

Number of molecules	Yield (%)
1	86
2	9
Multiple	5

Table S6. Assignment of SERS vibrations of ThT.

Peak position (cm ⁻¹)	Assignments ^{1, 2}
700	$\delta_I(\text{CCC})/\nu(\text{C}_6\text{SC})$
742	$\delta(\text{CCC})/\nu_s(\text{C}_6\text{SC})/\nu_s(\text{CN}_{18}\text{C})$
794	$\rho(\text{CH}_3)c_{11}/\delta(\text{CCC})$
1033	$\delta_I(\text{CCC})/\nu_{III}(\text{CC})$
1129	$\rho(\text{CH}_3)c_{11}/\delta_I(\text{CH})/\nu(\text{CC})/\nu(\text{CSC})/\nu(\text{NCC})$
1402	$\delta(\text{CH}_3)c_{11,10,19,20}/\delta_I(\text{CH})/\nu(\text{CC})$
1536	$\nu_{III}(\text{CC})/\nu(\text{C}_{15}\text{N}_{18})/\nu(\text{C}_6\text{C}_{12})/\delta(\text{CH}_3)c_{19,20}$
1600	$\nu_{III}(\text{CC})$

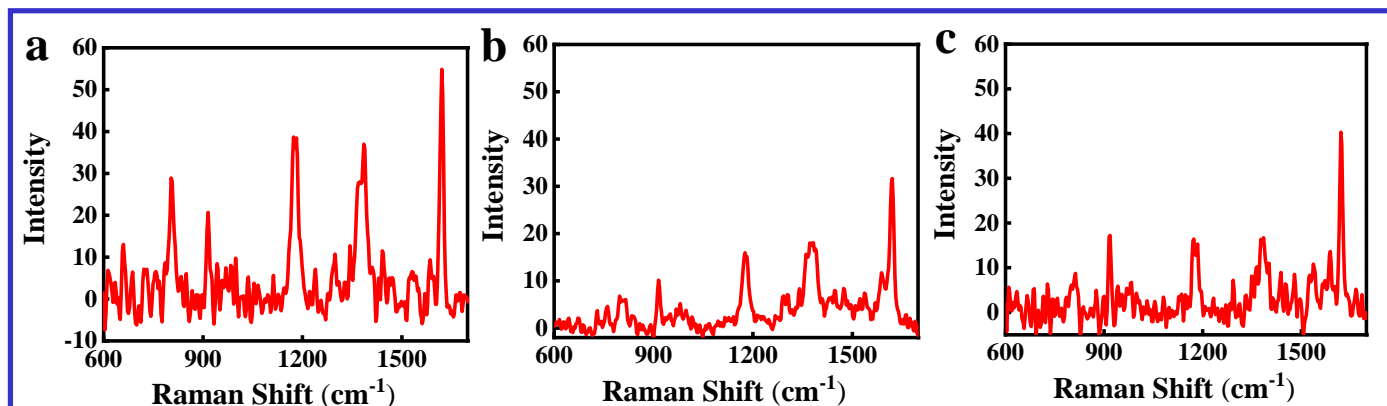


Figure S14. (a), (b), and (c) SERS spectra of ThT using Au NBPs dimer nanoantenna.

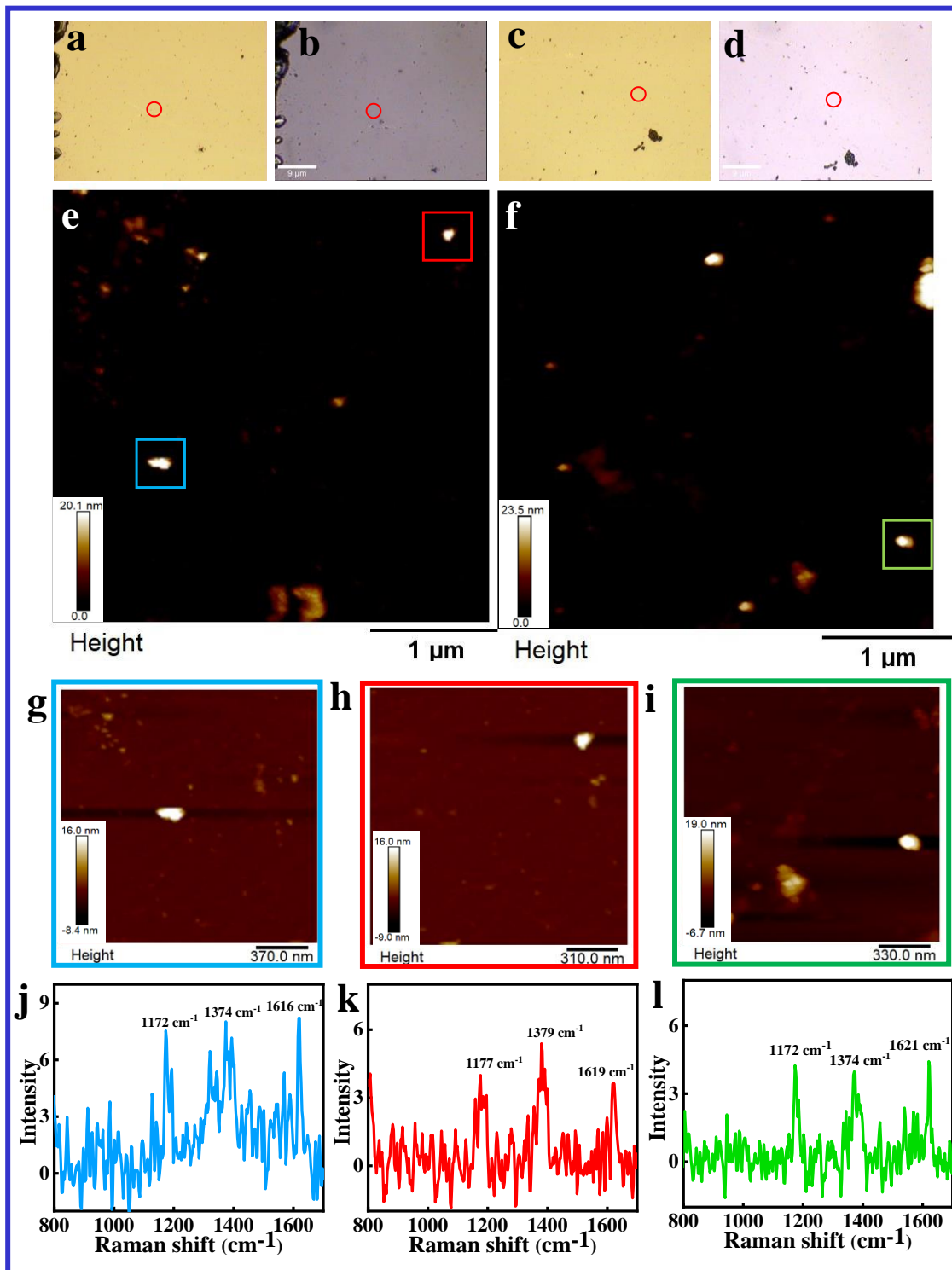


Figure S15. Single-molecule SERS measurements of ThT dye using Au NBPs nanoantenna. Optical image recorded using ((a), (c)) AFM, and ((b), (d)) confocal Raman microscopes (red circles show the scanned area), respectively ((e), (f)) AFM images, ((g), (h), and (i)) high resolution AFM image of a single nanoantenna structure, and ((j), (k), and (l)) their corresponding single-molecule SERS spectra.

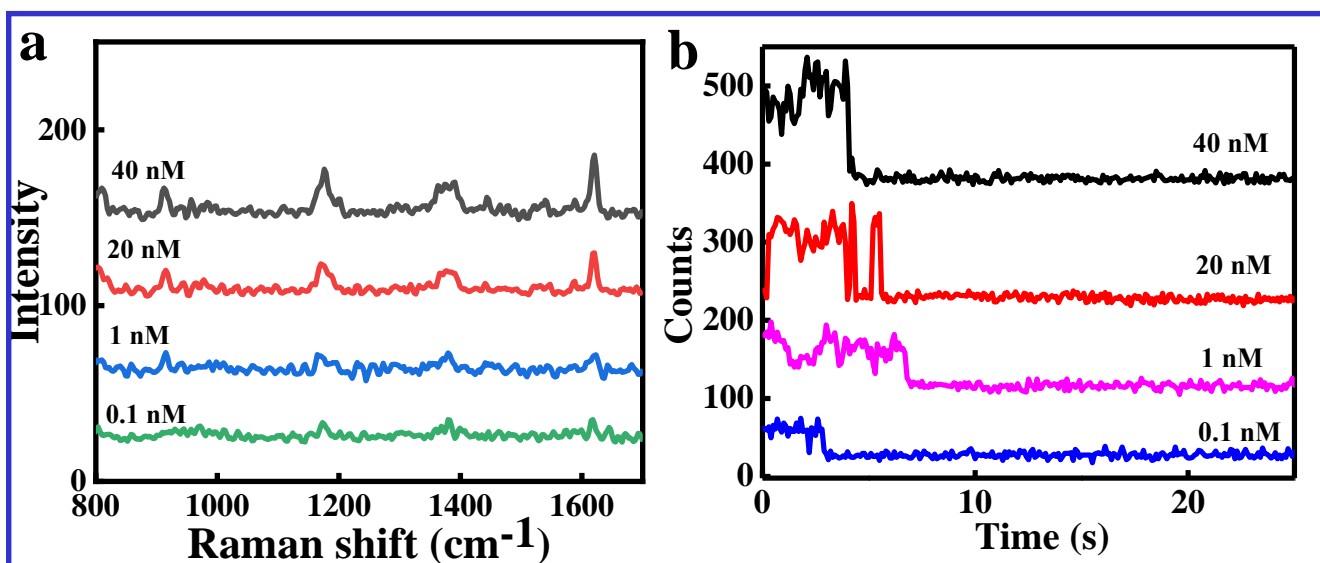


Figure S16. Concentration dependent (a) SERS, and (b) single molecule confocal fluorescence measurements of ThT dye using Au NBPs monomer.

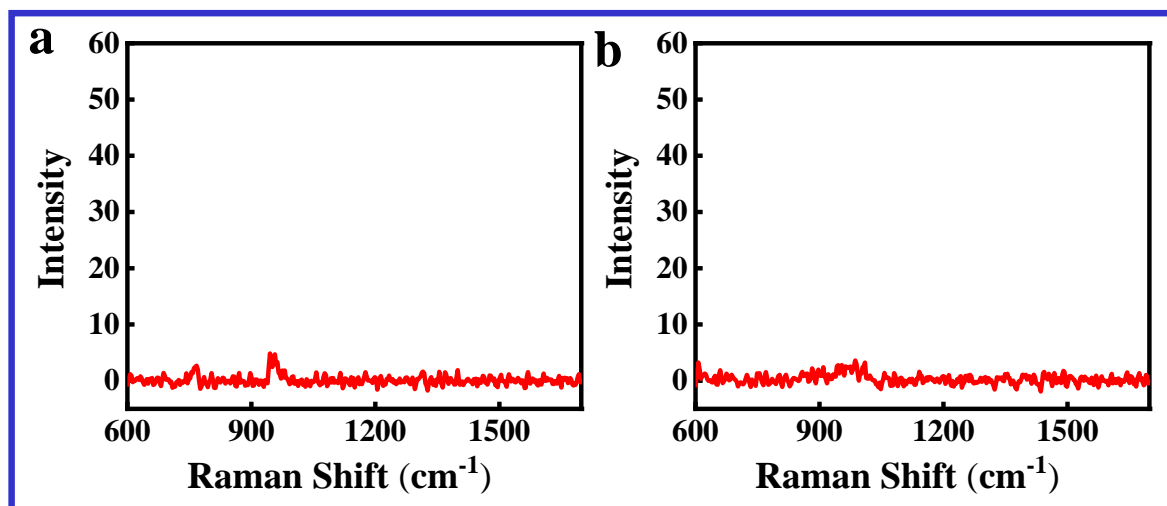


Figure S17. (a), and (b) Control Raman measurements using ThT on DNA origami (without Au NBPs).

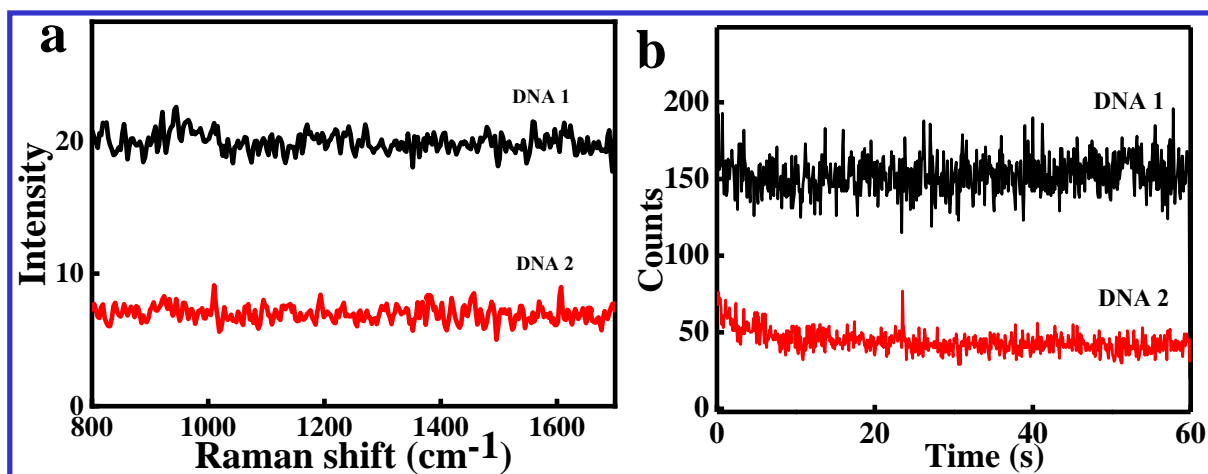


Figure S18. Control (a) Raman spectra, and (b) single molecule fluorescence time traces of ThT dye solution (0.1 nM) using different DNA sequences on DNA origami.

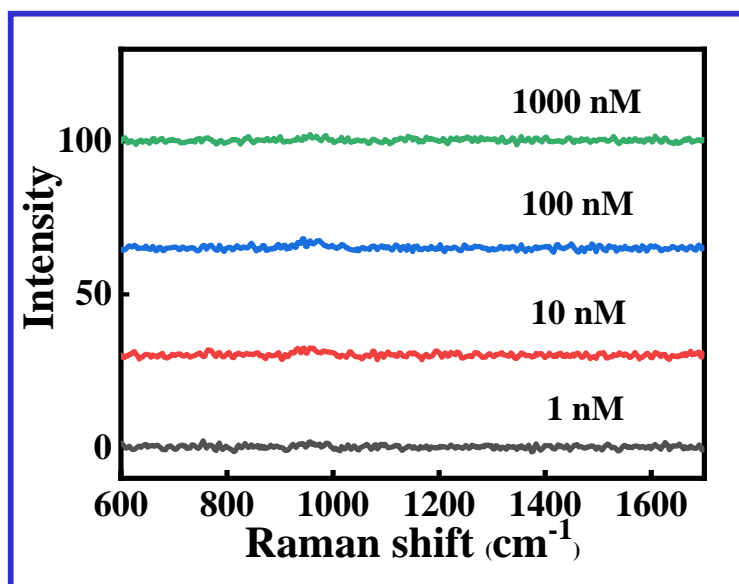


Figure S19. Raman measurements of different concentrations of ThT on Si wafer.

References

1. E. Lopez-Tobar, M. Antalík, D. Jancura, M. V. Cañamares, A. García-Leis, D. Fedunova, G. Fabriciova and S. Sanchez-Cortes, *The Journal of Physical Chemistry C*, 2013, **117**, 3996-4005.
2. N. Maiti, R. Chadha, A. Das and S. Kapoor, *Spectrochim Acta A Mol Biomol Spectrosc*, 2015, **149**, 949-956.